Spatio-temporal analysis of shoreline and migration of mangroves- A case study of Mandovi and Zuari estuaries including Cumbarjua Canal, Goa (2002-2022)

Deshpande Tanvi V.[1*] and Kerkar Pravina[2]
1. Government College of Arts, Science and Commerce, Khandola, Marcela, Goa, INDIA
2. Sant Sohirobanath Ambiye, Government College of Arts and Commerce, Virnoda, Pernem, Goa, INDIA
*tanvi.deshpande@khandolacollege.edu.in

Abstract

Mangroves are halophytes that are usually found in the inter-tidal regions in tropical and subtropical regions. Lush green and prominent patches of mangroves are found in Goa, especially in the Mandovi-Zuari-Cumbarjua estuarine complex. The present study aims to assess the shoreline changes along the selected estuaries of Goa and to study the landward migration of mangroves. OBIA Segmentation techniques have been implemented to map mangrove ecosystems over 20 years. From the spatio-temporal analysis (2002-2022), landward migration of mangroves has been observed in the selected estuaries-Mandovi and Zuari including Cumbarjua canal. To further understand the landward migration of mangroves, shoreline analysis has been carried out using DSAS tool. DSAS analysis has been carried out with respect to EPR as it is easy for computation and requires shorelines of two time periods for analysis.

From shoreline analysis, it has been understood that the accretion rate is dominant over the erosion rate. Overall, it has been observed that there is accretion and landward migration of mangroves, which can be attributed to the landward shift of mangroves irrespective of rise in sea level if there is availability of adequate sediment and landward space. Also availability of sediments resulting from heavy rainfall and runoff leads to sedimentation and allows growth of mangroves.

Keywords: Mangroves, Goa, landward migration, shoreline change, DSAS.

Introduction

Mangroves: Mangroves are salt-tolerant evergreen forest ecosystems found in the inter-tidal regions of tropics and sub-tropics approximately between 32^0N and 38^0S latitude[36]. Mangroves have submerged roots, trunks and branches[7]. Mangroves act as carbon assimilators[19] as they can store more carbon than that of the tropical forest ecosystem, thereby lowering the carbon dioxide concentration in the atmosphere[30].

Identification of mangroves: Mangroves have special habitat requirements and are usually located in inter-tidal zones and tidally inundated creeks and rivers[21, 38]. Mangroves can be differentiated from terrestrial and coastal vegetation based on tone (red, pale red), association (mudflats, warm waters, low energy coast) and location (intertidal areas)[29]. Mangroves are evergreen forests and exhibit green properties for the whole year, hence can be easily identified with visual interpretation[40]. Textural and spectral characteristics of the canopy and leaves are important characteristics used to differentiate between mangroves[6].

LANDSAT data: Landsat images have been extensively used to map and to study the coastal land cover giving good accuracy at different temporal resolution[4]. The five advantages of using medium-resolution imageries for mangrove studies are Landsat Thematic Mapper (TM), Enhanced Thematic Mapper (ETM+) and Operational Land Imager (OLI), which are universally used data sets for land classification. The first advantage is spatial resolution that ranges from 10m to 30m and can provide spatial extent of mangrove cover. The second advantage is abundant spectral bands which facilitate the identification of mangroves. The third advantage is consistency of the data availability every half month to 1 month, which helps to observe the mangrove extent. The fourth advantage is that of long historical records available at the world level and the fifth is affordability and easy accessibility of the images[17].

DSAS: Shorelines are dynamic and are defined as a distinct boundary between land and water[26]. In the latest times, remote sensing data has been expansively used in analysing shoreline change due to their synoptic and recurring coverage, high resolution, multispectral capabilities and is cost-effective in comparison to conservative techniques[5]. The DSAS has been used extensively to calculate the rate of shoreline changes. The Digital Shoreline Analysis System (DSAS) is a GIS-based system developed by the United States Geological Survey (USGS) and an extension to ArcMap and was introduced to automatically or manually generate measurements of transects and metadata based on user-specified parameters[32,39,42].

DSAS is a useful tool that helps in the analysis of historical trends of the present and past mangrove shoreline position measuring the changes at the casted transects from a defined baseline[32]. This study aims to assess the shoreline changes along the selected estuaries of Goa and study the associated migration of mangroves.

Study Area

The mangrove cover in Goa is approximately 0.5% of the total mangrove cover of India[24]. Mangroves are found along the estuaries of Terekhol, Chapora, Mandovi, Zuari, Sal, Talpona, Galgibag and Cumbarjua canal[35]. Most of the mangroves in Goa are fringing mangroves bordering the estuaries and creeks[18, 28]. Figure 1 represents a map of the study area.

Material and Methods

Materials: To fulfill the aim of the study, LANDSAT data series have been used. The LANDSAT data for the years 2002 and 2022 of 30 m spatial resolution with 0% cloud cover are acquired from the USGS website. Table 1 represents a detail listing of the satellite imageries and associated information. Figure 2 represents the methodology followed for generating the results.

Delineation of mangroves: The Object-based Image Analysis (OBIA) utilizes the phenomena of spectral brightness that is different for pixels representing different land cover types[20]. The object-based method is composed of two phases: 1) image segmentation and 2) extraction of features and classification[16, 23, 34, 37]. Segmentation provides the building blocks of object-based image analysis[8]. The image segmentation process is the basic and important step of object-based image analysis (OBIA). The segmentation process divides or splits the image into spatially continuous, mutually disconnected and homogenous regions called objects based on specified parameters defined by the user, spectral information and shape which coincide with the actual spatial pattern[9,10, 25,27,43].

In the current study, the segmentation process has been carried out using ArcGIS 10.3 software using the Segment Mean Shift Tool. Mangroves are identified by visual interpretation techniques viz. location, texture, tone, association and with the help of high-resolution Google Earth system. Further validation has been done through ground truthing. Spatio-temporal analysis of mangroves has been carried out for the years 2002 and 2022 i.e. for 20 years.

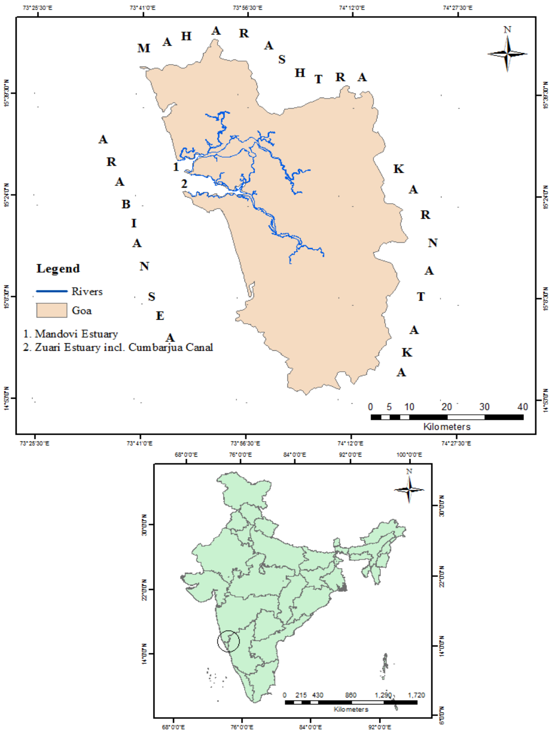

Figure 1: Map of Study Area

Table 1
Data derived from satellite images

Data used	Date of Acquisition	Path and Row	Total no. of Bands	FCC Band Composition	Data generated
LANDSAT 7 ETM+ (2002)	06/01/2002 15/01/2002 15/01/2002	147, 49 146, 49 146, 50	08	4, 3, 2	mangrove and shorelines delineation
LANDSAT 8 OLI (2022)	30/01/2022 30/01/2022 06/02/2022	146, 49 146, 50 147, 49	11	5, 4, 3	

https://doi.org/10.25303/178da08017

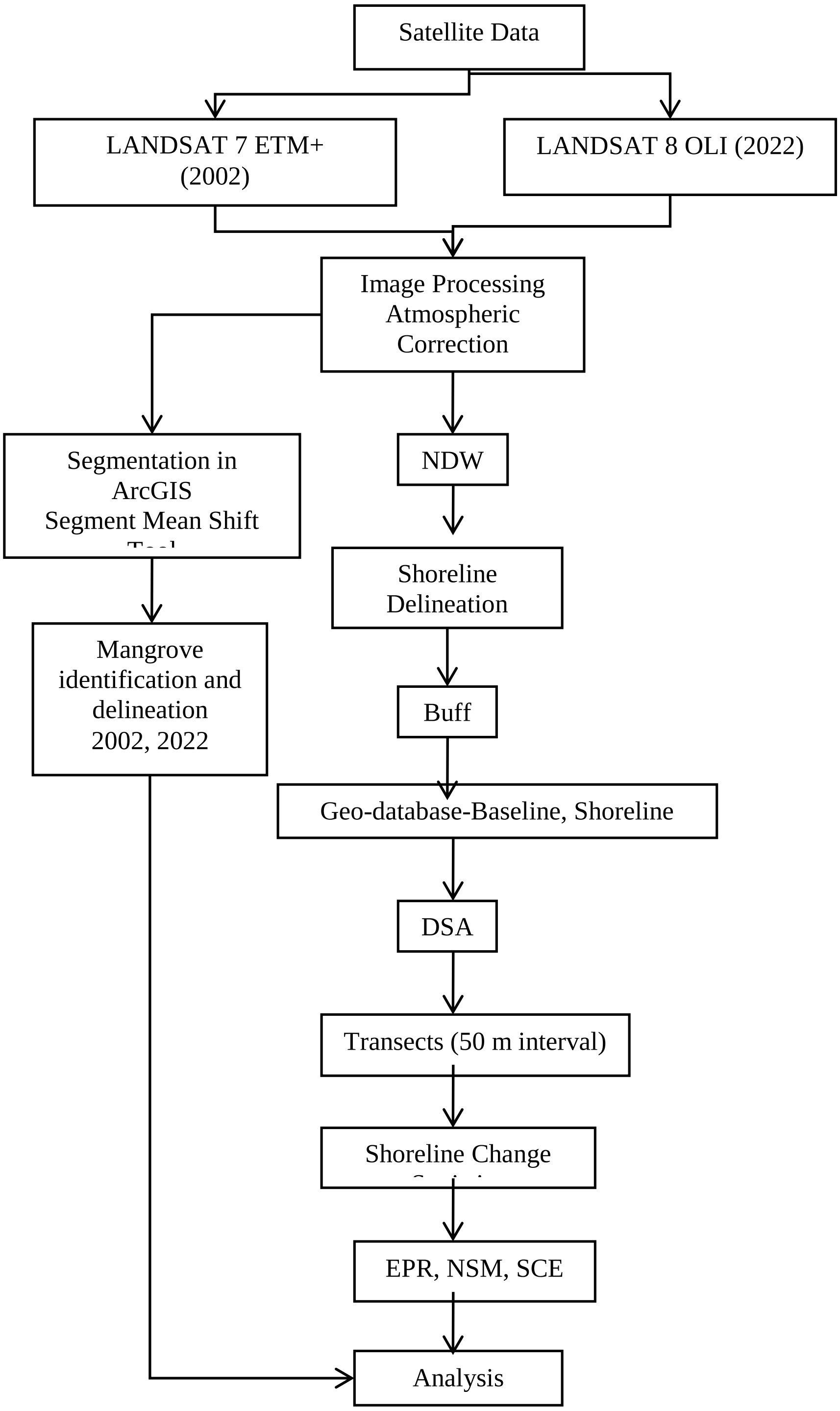

Figure 2: Methodology

Table 2
Band information

Data used	Band Information	Formula
LANDSAT 7 ETM+ (2002)	NIR-4, Green-2	NDWI= Green-NIR/ Green+NIR
LANDSAT 8 OLI (2022)	NIR-5, Green-3	

Delineation of shoreline and DSAS analysis: Several studies have used the spectral indices to map the shoreline and the most important indicator used is the NDWI[2]. Shorelines for the year 2002 and 2022 are manually digitized with the help of the NDWI index. Table 2 shows the bands used for calculating NDWI.

DSAS v5.0 is used for shoreline analysis which is an extension tool of Arc GIS. DSAS calculates gaps between the shoreline positions during defined periods. This provides the fundamental data to estimate the shoreline changes[39]. The software is designed to aid the shoreline change-calculation process and also to give a rate of change information[5]. The DSAS requires the following inputs (a) multiple shorelines of different time series (b) a user-generated baseline (c) DSAS generates transects which are cast perpendicular to the baseline at a user-defined spacing. These transects along the baseline are used to calculate the rate-of-change statistics. There are various methods to calculate the shoreline change such as Shoreline Change Envelope (SCE), Net Shoreline Movement (NSM), End Point Rate (EPR) and Linear Regression Rate (LRR), Weighted Linear Regression Rate (WLR), Least Median of Squares (LMS). In the present study, shorelines for two time periods are analysed i.e. 2002 and 2022. The current shoreline analysis involved statistical parameters such as Shoreline Change Envelope (SCE), Net Shoreline Movement (NSM) and End Point Rate (EPR)[5,22].

Using Arc GIS 10.3 software, the two shorelines (2002, 2022) are merged and a buffer of 50 m was produced to generate the baseline. A baseline is a reference datum used in the DSAS model which serves as a starting point to cast transects at the closest intersection with shorelines using a simple baseline cast method, crossing through the individual shoreline vectors and providing statistical measures of change over time. For generating a baseline in the ArcGIS geodatabase, five attribute fields are required which include object ID (a unique number assigned to each transect), shape (polyline), shape length, ID and cast direction. Similarly, for shorelines geodatabase, three attribute fields are included namely- shape length, date and uncertainty.

Transects have been generated at a length of 200 m from the baseline towards the land with a 50 m spacing interval between them. Transects generated on the baseline intersect the shoreline at the specified distance which is used to calculate shoreline change rates. Further, analysis of the shoreline changes through processes of accretion and erosion has been done by basic statistical techniques from the derived DSAS results.

Results and Discussion

Temporal analysis of mangroves: It has been observed that over the last 20 years, there has been an increase in mangrove cover in Mandovi Zuari including Cumbarjua canal by 14.79 km^2 and 8.58 km^2 respectively. Table 3 depicts the spatio-temporal changes in mangrove cover for 20 years. The increase in mangrove cover can be attributed to the natural regeneration of mangroves and plantation drives taken up by the forest department and NGOs. The mangroves in Goa have increased continuously from 1973 to 2011, with the largest gain occurring from 2006 to 2011[13]. Chorao island in the estuarine region of Mandovi River has a thick mangrove cover. In 1988, the Government of Goa declared this mangrove forest as protected and conserved and is named Dr. Salim Ali bird sanctuary.

From the maps, it can be identified that there is a landward migration of mangroves. Figure 3 represents the spatio-temporal changes in mangrove cover from 2002-2022. In Mandovi River, Nerul, Ribandar, Patto, Divar Island, Narve, Calvim, Aldona, Amona etc. have landward migration of mangroves. Cumbarjua landward migration of mangroves is observed. To further understand the landward migration of mangroves, shoreline analysis has been carried out using the DSAS tool.

Shoreline analysis: End Point Rate (EPR) gives the rate of change of shoreline movement which is calculated by dividing the distance of shoreline movement by the time elapsed between the oldest and the most recent shoreline. The negative rate values indicate erosion, movement of the shoreline landwards whereas the positive rate values indicate accretion i.e. movement of the shoreline towards the sea[1,32,39]. In the current study, the oldest shoreline was from the year 2002 while the most recent shoreline was from 2022. The chief advantage of the EPR is its ease of computation and minimal requirements for shoreline data i.e. EPR calculation requires only two shorelines for computation unlike LRR, WLR and LSM[33].

The EPR is expressed using the following equation 1:

$$EPR = D1-D2/\ t1-t2 \qquad (1)$$

where D1−D2 is the distance between the oldest and youngest coastlines and t1 and t2 are the dates of the oldest and youngest coastlines. The EPR parameter gives an overall change throughout the period since it depends on the oldest and youngest coastlines[31].

Table 3
Spatio-temporal changes in Mangrove cover (2002-2022)

S.N.	River	Area in 2002 (km^2)	Area in 2022 (km^2)
1	Mandovi	10.61	25.4
2	Zuari incl. Cumbarjua Canal	9.35	17.93

Table 4
Shoreline Change Envelope

SCE (Shoreline Change Envelope) in meters			
Estuaries	**Average Distance (m)**	**Maximum distance (m)**	**Maximum Distance Transect ID**
Mandovi	24.65	159.59	133
Zuari including Cumbarjua Canal	18.26	178.22	271

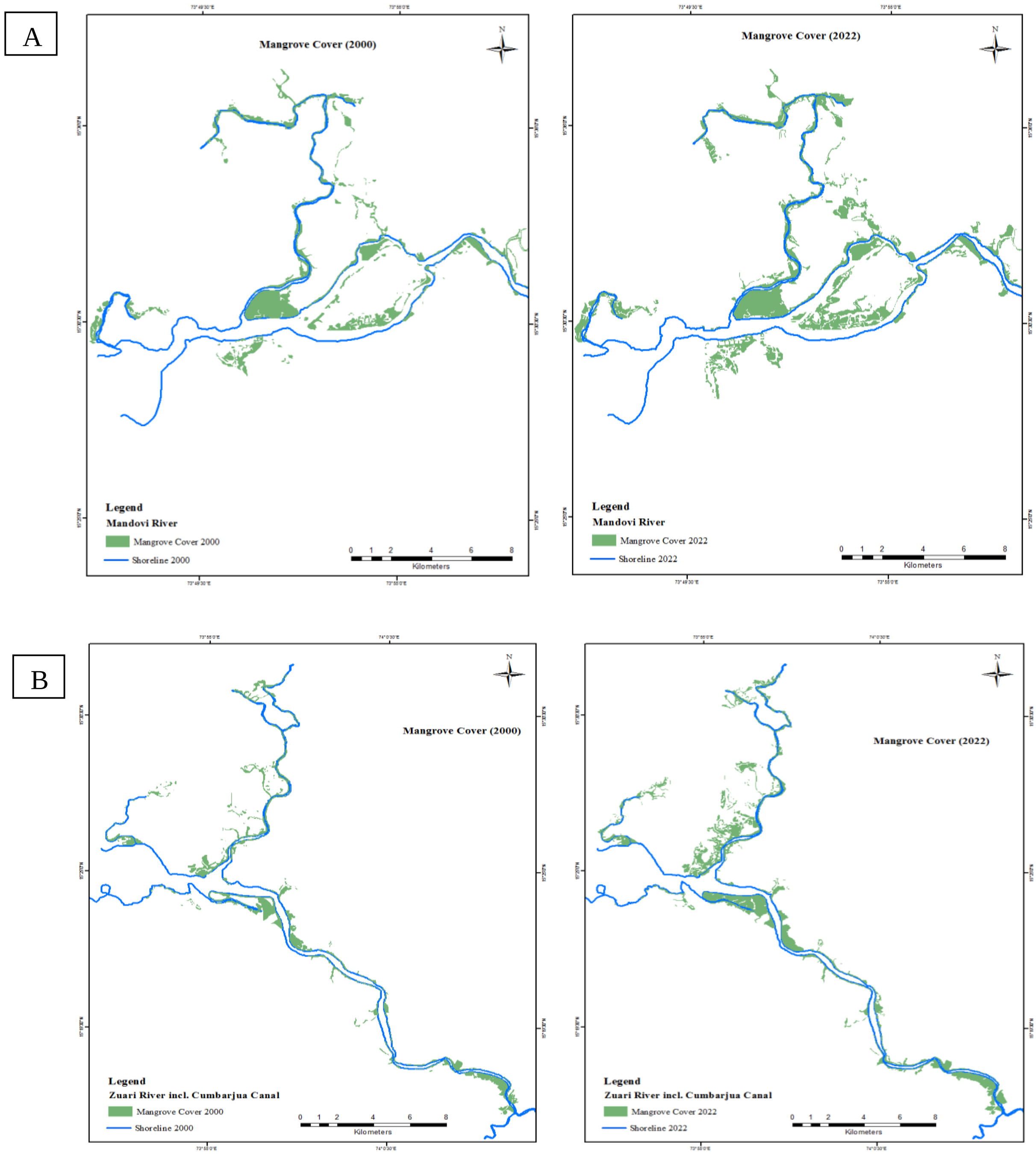

Figure 3: Temporal changes in mangrove cover from 2002-2022
A) Mandovi river, B) Zuari river including Cumbarjua Canal

Table 5
Net Shoreline Movement

NSM (Net Shoreline Movement) in meters						
Estuaries	**Maximum Positive distance (m)**	**Maximum Positive distance Transect ID**	**Average of all positive distances (m)**	**Maximum Negative distance (m)**	**Maximum Negative distance Transect ID**	**Average of all negative distances (m)**
Mandovi	159.59	133	26.3	-99.97	126	-10.03
Zuari incl. Cumbarjua Canal	164.67	236	14.54	-178.22	271	-25.15

Table 6
End Point Rate-Accretion

Accretion- EPR (End Point Rate) in meters/year							
Estuaries	**Total Transects**	**No. of Accretion Transects**	**% of Accretion Transects**	**Overall Accretion (m) (2002-2022)**	**Maximum value of Accretion (m/yr)**	**Maximum value of Accretion Transect ID**	**Average of all Accretion Rates (m/yr)**
Mandovi	1880	1690	89.89	2191.97	7.95	133	1.29
Zuari including Cumbarjua Canal	1772	1143	64.5	846.39	8.21	236	0.7

Table 7
End Point Rate-Erosion

Erosion- EPR (End Point Rate) in meters/year							
Estuaries	**Total Transects**	**No. of Erosion Transects**	**% of Erosion Transects**	**Overall Erosion (m) (2002-2022)**	**Maximum value of Erosion (m/yr)**	**Maximum value of Erosion Transect ID**	**Average of all Erosion Rates (m/yr)**
Mandovi	1880	190	10.1	-95.27	-4.98	126	-0.5
Zuari including Cumbarjua Canal	1772	629	35.49	-792.24	-8.88	271	-1.25

Net shoreline movement (NSM) is described as the distance between the oldest and the most recent shoreline along a transect that has been considered[14]. Tables 4, 5, 6 and 7 represent the statistical analysis of shoreline change analysis.

Both river shoreline analyses represent maximum deposition which can be observed from the difference between number of transects generated for accretion and erosion respectively. In the case of Mandovi river, 1690 transects represent accretion while only 190 transects represent erosion which are 89.89% and 10.1% of accretion and erosion. Maximum accretion is 7.95 m/yr while maximum erosion is -4.98 m/yr. From 2002-2022, overall accretion and erosion noted are 2191.97 m and -95.27 m respectively. Maximum positive and negative NSM are 159.59 m and -99.97 m respectively.

Out of a total of 1772 transects generated for the Zuari river including the Cumbarjua Canal, 1143 transects represent accretion and 629 transects represent erosion which are 64.5% and 35.49% of accretion and erosion respectively. Maximum accretion is 8.21 m/yr while maximum erosion is -8.88 m/yr. From 2002-2022, overall accretion and erosion noted are 846.39 m and -792.24 m respectively. Maximum positive and negative NSM are 164.67 m and -178.22 m respectively. Figures 4 and 5 show graphical representation of EPR and NSM.

Figures 6 and 7 represent the shoreline change and mangrove spatial extent. Prominent accretion and landward migration of mangroves in Mandovi River have been observed at St. Estevam, Vanxim Island, Chorao Island, Salvador-Do-Mundo etc. In Zuari river, Adpai, Quelossim, Rachol and Curtorim have prominent accretion and landward migration of mangroves.

Mangrove ecosystems being dynamic can migrate landward when considering the effect of sea level rise[11]. However, Xie et al[44] stated that there can be an increase in mangrove cover regardless of sea-level rise if sediment supply is adequate and landward space is available. Higher rainfall can supply greater organic matter and detritus-rich fluvial sediment and hence can increase mangrove productivity and diversity until a maximum threshold[3,12].

Mangroves flourish in regions where the annual mean precipitation is approximately 1500–3000 mm as they benefit from heavy runoff and discharge from river systems resulting in sedimentation. These conditions are therefore likely to lead to increased productivity of mangroves and changes in diversity, structure and extent[3].

Tomlinson[41] stated that richer species of mangroves exist along the regions of high rainfall and heavy runoff leading to extensive sedimentation.

The overall annual rainfall in the State of Goa based on the last 30 years' rainfall data is 3483.3mm[15]. In addition, accretion has been dominant rather than erosion rate which can be associated with high rainfall and resultant heavy runoff causing sedimentation. Hence, it can be concluded that there is an increase in mangroves along with landward migration due to sedimentation. The elevation also plays an important role in the landward migration of mangroves. The mangroves along the estuaries of Goa are fringing mangroves that lie in low elevation zones along the estuaries. Due to low elevation or flat surface, inward migration of mangroves is likely to occur as there is no obstruction for inward growth.

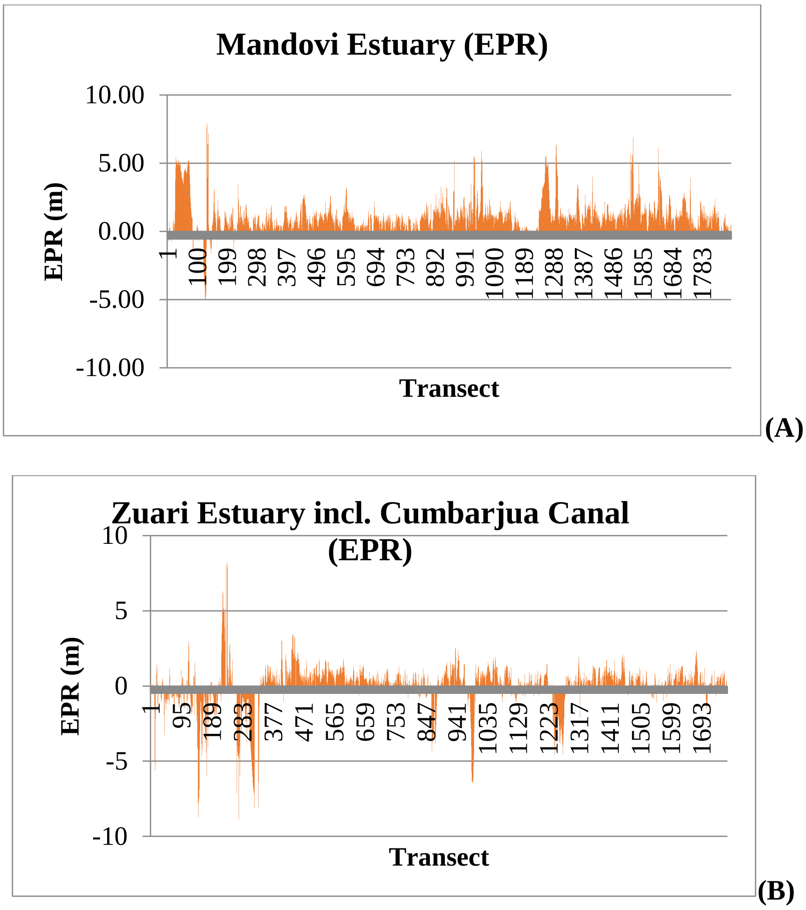

Figure 4: End Point Rate (2002-2022): A) Mandovi river, B) Zuari river including Cumbarjua Canal

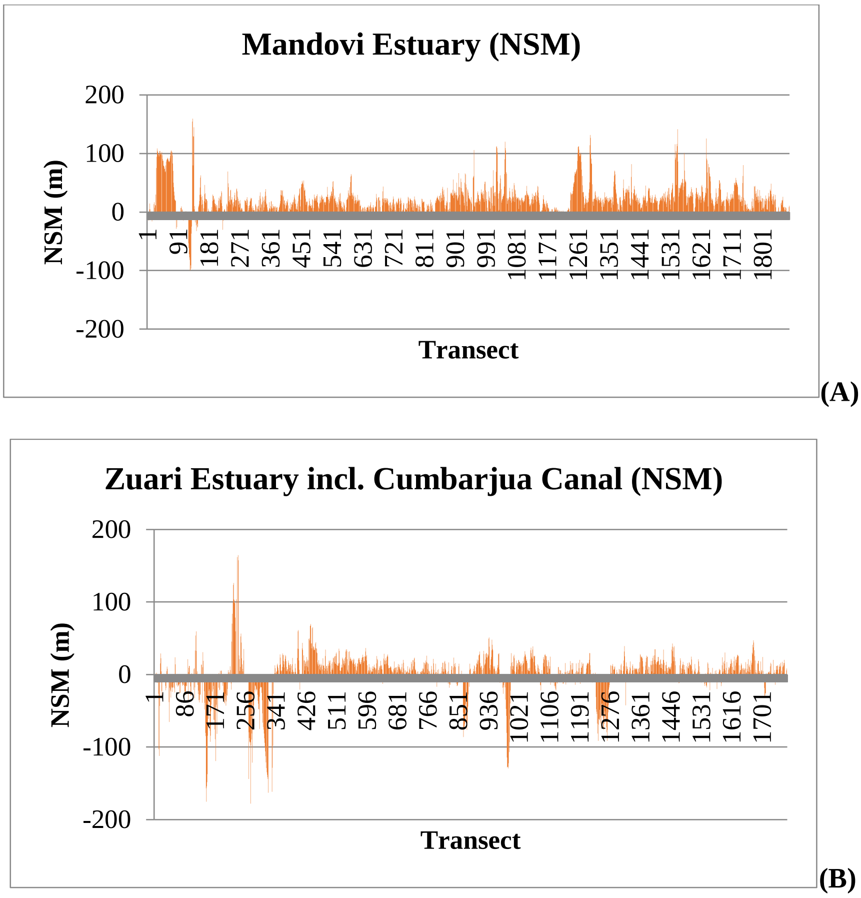

Figure 5: Net Shoreline Movement (2002-2022): A) Mandovi Estuary, B) Zuari Estuary including Cumbarjua Canal

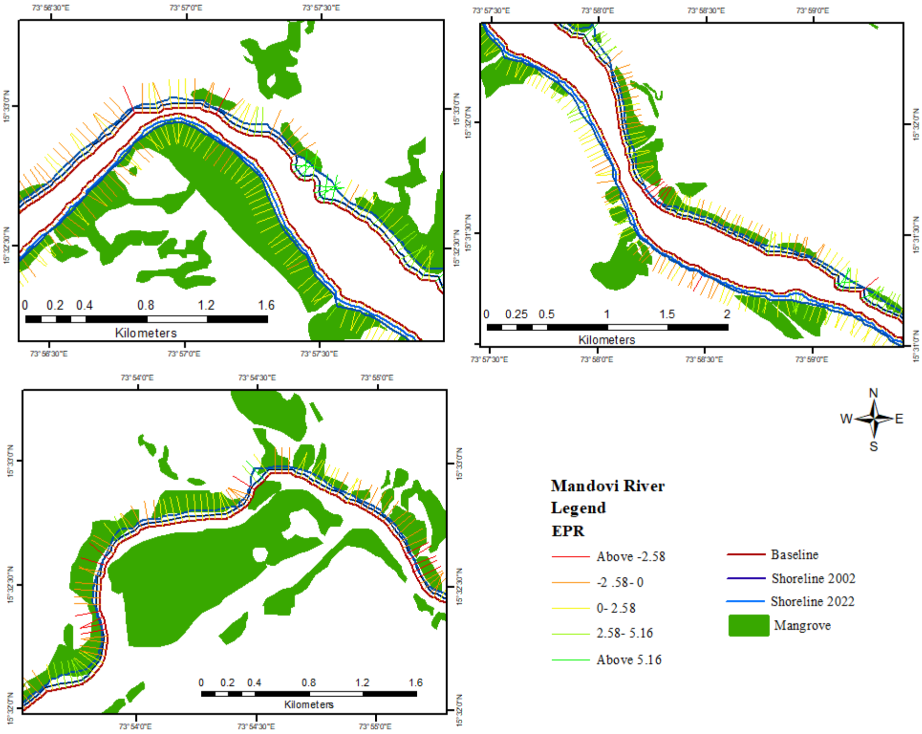

Figure 6: Shoreline change and mangrove spatial extent in Mandovi Estuary

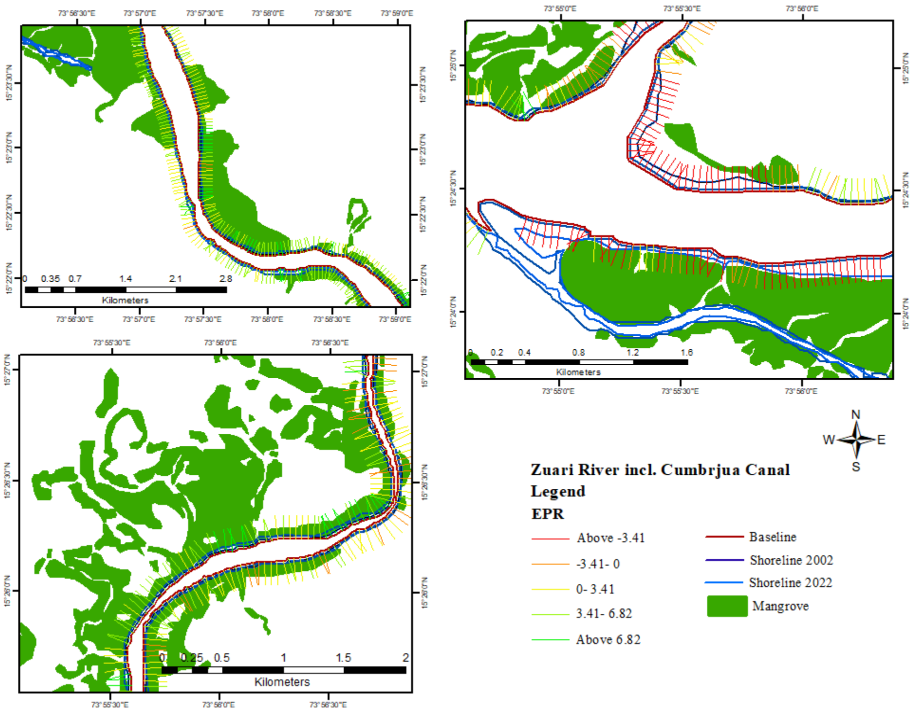

Figure 7: Shoreline change and mangrove spatial extent in Zuari Estuary including Cumbarjua Canal

Conclusion

Over the last 20 years, increase in mangrove cover in Mandovi is by 14.79 km^2 and in Zuari including Cumbarjua canal it is 8.58 km^2. The increase in mangrove cover can be attributed to the natural regeneration of the mangroves and also to the plantation drives taken up by the forest department and NGOs. The rate of accretion is more dominant than the rate of erosion. Hence, landward migration of mangroves has been observed in many regions and can be associated with the dynamic nature of mangroves and excess sediment supply where mean annual rainfall is approximately 1500–3000 mm. Low elevation along the estuaries also favours the inward growth of mangroves due to no obstruction.

References

1. Ahammed B. and Pandey A.C., Assessment and prediction of shoreline change using multi-temporal satellite data and geostatistics: A case study on the eastern coast of India, *Journal of Water and Climate Change*, **13(3)**, 1477-1493 **(2022)**

2. Albanai J.A., Sea level rise projections for Failaka Island in the State of Kuwait, *Transactions on Maritime Science*, **9(2)**, 236-247 **(2020)**

3. Asbridge E., Lucas R., Accad A. and Dowling R., Mangrove response to environmental changes predicted under varying climates: case studies from Australia, *Curr. Forestry Rep.*, **1**, 178–194 **(2015)**

4. Avtar R., Navia M., Sassen J. and Fujii M., Impacts of changes in mangrove ecosystems in the Ba and Rewa deltas, Fiji using multi-temporal Landsat data and social survey, *Coastal Engineering Journal*, **63(3)**, 386-407 **(2021)**

5. Baig I., Ahmad I., Shahfahad A., Tayyab M. and Rahman A., Analysis of shoreline changes in Vishakhapatnam coastal tract of Andhra Pradesh, India: an application of digital shoreline analysis system (DSAS), *Annals of GIS*, **26(4)**, 361-376 **(2020)**

6. Baloloy A.B., Blanco A.C., Sharma S. and Nadaoka K., Development of a rapid mangrove zonation mapping workflow using sentinel 2-derived indices and biophysical dataset, *Front. Remote Sens.*, **2**, 1-18 **(2021)**

7. Basheer M.A., El Kafrawy S.B. and Mekawy A.A., Identification of mangrove plant using hyperspectral remote sensing data along the Red Sea, Egypt, *Egyptian Journal of Aquatic*, **23(1)**, 27 – 36 **(2019)**

8. Blaschke T., Object based image analysis for remote sensing, *ISPRS Journal of Photogrammetry and Remote Sensing*, **65**, 2–16 **(2010)**

9. Concheddaa G., Durieux L. and Mayaux P., An object-based method for mapping and change analysis in mangrove ecosystems, *ISPRS Journal of Photogrammetry & Remote Sensing*, **63**, 578–589 **(2008)**

10. Das B. and Dhorde A., Geostatistical approach to assess mangrove spatial variability: a bi-decadal scenario over Raigarh coast of Maharashtra, *Journal of Coastal Conservation*, **25(1)**, Doi: 10.1007/s11852-021-00813-8 **(2021)**

11. Di Nitto D., Neukermans G., Koedam N., Defever H., Pattyn F., Kairo J.G. and Dahdouh-Guebas F., Mangroves facing climate change: landward migration potential in response to projected scenarios of sea level rise, *Biogeosciences Discuss*, **10**, 3523–3558 **(2013)**

12. Ellison J., Chapter 15: How South Pacific mangroves may respond to predicted climate change and sea level rise, Climate Change in the South Pacific: impacts and responses in Australia, New Zealand and Small Islands States, Dordrecht: Kluwer Academic **(2000)**

13. Giri C., Long J., Abbas S., Mani Murali R., Qamer F.M., Pengra B. and Thau D., Distribution and dynamics of mangrove forests of South Asia, *Journal of Environmental Management*, **148**, 101-111 **(2014)**

14. Gopinath G., Thodi M.F.C., Surendran U.P., Prem P., Parambil J.N., Alataway A., Al-Othman A.A., Dewidar A.Z. and Mattar M.A., Long-term shoreline and islands change detection with digital shoreline analysis using RS data and GIS, *Water*, **15(2)**, https://www.mdpi.com/2073-4441/15/2/244 **(2023)**

15. Government of India Ministry of Water Resources, River Development & Ganga Rejuvenation, Central Ground Water Board, Ground Water Year Book Goa State, 2015-16 **(2016)**

16. Hossain M.D. and Chen D., Segmentation for Object-Based Image Analysis (OBIA): A review of algorithms and challenges from remote sensing perspective, *ISPRS Journal of Photogrammetry and Remote Sensing*, **150**, 115-134 **(2019)**

17. Hu L., Li W. and Xu B., The role of remote sensing on studying mangrove forest extent change, *International Journal of Remote Sensing*, **39(19)**, 6440-6462 **(2018)**

18. Jagtap T.G., Naik S. and Nagle V.L., Assessment of coastal wetland resources of Central West Coast, India, using LANDSAT Data, *Journal of the Indian Society of Remote Sensing*, **29(3)**, 140-150 **(2001)**

19. Kamboj R.D. and Das L., The dynamics of mangrove cover in India based on assessment done by Forest Survey of India from 1987 to 2017, *Indian Forester*, **145(7)**, 607-613 **(2019)**

20. Lemenkova P., Object based image segmentation algorithm of SAGA GIS for detecting urban spaces in Yaoundé, Cameroon, *Central European Journal of Geography and Sustainable Development*, **2(2)**, 38-51 **(2020)**

21. Long B.G. and Skewes T.D., A technique for mapping mangroves with landsat TM satellite data and geographic information system, *Estuarine, Coastal and Shelf Science*, **43**, 373–381 **(1996)**

22. Mahapatra M., Ratheesh R. and Rajawat A.S., Shoreline change analysis along the coast of South Gujarat, India, using digital shoreline analysis system, *J. Indian Soc. Remote Sens.*, **42**, 869–876 **(2014)**

23. Maurya K., Mahajan S. and Chaube N. Remote sensing techniques: mapping and monitoring of mangrove ecosystem—a review, *Complex & Intelligent Systems*, **7**, 2797–2818 **(2021)**

24. Mesta P.N., Setturu B., Subash Chandran M.D., Rajan K.S. and Ramachandra T.V., Inventorying, mapping and monitoring of mangroves towards sustainable management of West Coast, India, *J. Geophys. Remote Sensing*, **3**, DOI: 10.4172/2169-0049.1000130 **(2014)**

25. Mohan Vamsee A., Kamala P., Martha T.R., Vinod Kumar K., Jaisankar G. and Amminedu E., A tool assessing optimal multi-scale image segmentation, *J. Indian Soc. Remote Sens.*, **46**, 31-41 **(2017)**

26. Mondal I., Thakur S., Juliev M., Bandyopadhyay J. and De T.K., Spatio-temporal modelling of shoreline migration in Sagar

Island, West Bengal, India, *Journal of Coastal Conservation*, **24(50)**, DOI:10.1007/s11852-020-00768-2 **(2020)**

27. Myint S.W., Giri C.P., Wang L., Zhu Z. and Gillette S.C., Identifying mangrove species and their surrounding land use and land cover classes using an object-oriented approach with a lacunarity spatial measure, *GIScience & Remote Sensing*, **45(2)**, 188-208 **(2008)**

28. Nagi H.M., Rodrigues R.S., Mani Murali R. and Jagtap T.G., Using remote sensing and GIS techniques for detecting land cover changes of mangrove habitats in Goa, India, *Faculty of Science Bulletin*, **26**, 21-33 **(2014)**

29. Nayak S. and Bahuguna A., Application of remote sensing data to monitor mangroves and other coastal vegetation of India, *Indian Journal of Marine Sciences*, **30(4)**, 195-213 **(2001)**

30. Parida B.R. and Kumar P., Mapping and dynamic analysis of mangrove forest during 2009–2019 using landsat–5 and sentinel–2 satellite data along Odisha Coast, *Tropical Ecology*, **61**, 538- 549 **(2020)**

31. Quang D.N., Ngan V.H., Tam H.S., Viet N.T., Tinh N.X. and Tanaka H., Long-term shoreline evolution using DSAS technique: A case study of Quang Nam Province, Vietnam, *J. Mar. Sci. Eng.*, **9(10)**, 1124 **(2021)**

32. Sharma G. and Patnaik K.V.K.R.K., Assessment of Coringa Mangrove shoreline migration using geospatial techniques, *Journal of Operational Oceanography*, **15(2)**, 126-135 **(2020)**

33. Sheik M. and Chandrasekar, A shoreline change analysis along the coast between Kanyakumari and Tuticorin, India, using digital shoreline analysis system, *Geo-spatial Information Science*, **14(4)**, 282-293 **(2011)**

34. Silalahi R.P., Jaya N.S., Tiryana T. and Mulia F., Assessing the crown closure of Nypa on UAV images using mean-shift segmentation algorithm, *Indonesian Journal of Electrical Engineering and Computer Science*, **9(3)**, 722-730 **(2018)**

35. Singh I.J., Singh S.K., Kushwaha S.P.S., Subhash Ashutosh and Singh R.K., Assessment and monitoring of estuarine mangrove forests of Goa using satellite remote sensing, *Journal of the Indian Society of Remote Sensing*, **32(2)**, 167-174 **(2004)**

36. Singh J.K., Structural characteristics of mangrove forest in different coastal habitats of Gulf of Khambhat arid region of Gujarat, west coast of India, *Heliyon*, **6(8)**, e04685 **(2020)**

37. Son N.T., Chen C.F., Chang N.B., Chen C.R., Chang L.Y. and Thanh B.X., Mangrove mapping and change detection in Ca Mau Peninsula, Vietnam, using landsat data and object-based image analysis, *IEEE Journal of Selected Topics in Applied Earth Observations and Remote Sensing*, **8(2)**, 503-510 **(2015)**

38. Song X.F., Cui H.S. and Guo Z.H., Remote sensing of mangrove wetlands identification, *Procedia Environmental Sciences*, **10**, 2287-2293 **(2011)**

39. Thinh N.A. and Hens L., A Digital Shoreline Analysis System (DSAS) applied on mangrove shoreline changes along the Giao Thuy Coastal area (Nam Dinh, Vietnam) during 2005-2014, *Vietnam Journal of Earth Sciences*, **39(1)**, 87-96 **(2017)**

40. Tieng T., Sharma S., MacKenzie R.A., Venkattappa M., Sasaki N.K. and Collin A., Mapping mangrove forest cover using landsat-8 imagery, sentinel-2, very high resolution images and google earth engine algorithm for entire Cambodia, IOP Conf. Series: Earth and Environmental Science **(2019)**

41. Tomlinson P.B., The botany of mangroves, Cambridge, Cambridge University Press **(1986)**

42. Tran Thi V., Tien Thi Xuan A., Phan Nguyen H., Dahdouh-Guebas F. and Koedam N., Application of remote sensing and GIS for detection of long-term mangrove shoreline changes in Mui Ca Mau, Vietnam, *Biogeosciences*, **11**, 3781–3795 **(2014)**

43. Wang L., Sousa W.P. and Gong P., Integration of object-based and pixel-based classification for mapping mangroves with IKONOS imagery, *International Journal of Remote Sensing*, **25(24)**, 5655-5668 **(2004)**

44. Xie D., Schwarz C., Brückner M.Z.M., Kleinhans M.G., Urrego D.H., Zeng Zhou Z. and van Maanen B., Mangrove diversity loss under sea-level rise triggered by bio-morphodynamic feedbacks and anthropogenic pressures, *Environmental Research Letters*, **15**, DOI 10.1088/1748-9326/abc122 **(2020)**

(Received 08th March 2024, accepted 06th May 2024)